

High-Resolution Imaging of a Dislocation on Cu(111)

A. Samsavar, E. S. Hirschorn, T. Miller, F. M. Leibsle, J. A. Eades, and T.-C. Chiang

*Department of Physics, University of Illinois at Urbana-Champaign,
1110 West Green Street, Urbana, Illinois 61801*

*and Materials Research Laboratory, University of Illinois at Urbana-Champaign,
104 South Goodwin Avenue, Urbana, Illinois 61801*

(Received 3 November 1989)

A dislocation emerging on a Cu(111) surface was studied by scanning tunneling microscopy. The Burgers vector and the resulting lateral and vertical shifts in atomic positions were determined. The dislocation was found to consist of two partial dislocations separated by 25 Å.

PACS numbers: 68.55.-a, 61.16.Di, 61.50.Cj

Studies of imperfections in solids, especially dislocations, have been an important area of materials research. Dislocations play a central role in the mechanical properties and growth behaviors of crystalline solids.¹⁻⁵ An elementary account of the connection between dislocations and physical properties such as plastic deformation, slip, grain-boundary formation, and ledge growth can be found in, for example, Kittel's textbook on solid-state physics.⁶ Over the past fifty years or so, there has been continuing improvement and development in the experimental techniques for direct observation of dislocation structures. With the advent of high-resolution microscopy techniques, the interest has been focused on the detailed atomic structure near the core region where the atomic positions are significantly distorted relative to the periodic crystal structure.

Bulk dislocations have been extensively studied in the past with transmission electron microscopy (TEM), which has provided a detailed understanding of the structural properties.⁷ Other techniques, such as field-ion and field-emission microscopy and reflection electron holography and microscopy, have also been demonstrated to yield complementary information.^{8,9} The present work is a scanning-tunneling-microscopy (STM) study of a bulk dislocation emerging on a Cu(111) surface.¹⁰ Although bulk dislocations in fcc metals, Cu in particular, have been studied in detail by TEM, the atomic structure of a single bulk dislocation terminating on an otherwise flat single-crystal Cu(111) surface has not been reported before. From a direct viewing of the surface atomic positions, our results show that the dislocation consists of a pair of partial dislocations separated by about 25 Å, in excellent agreement with an earlier TEM study of a bulk dislocation in Cu.¹¹ This study demonstrates the usefulness of STM as another microscopy tool for dislocation studies. The interaction between surfaces (e.g., reconstructions) and dislocations would be a suitable area of application. The technique is quite attractive in that the interpretation of the image is simple and intuitive (for simple metal surfaces, each protrusion corresponds to a surface atom, and the image resembles a

photograph).

The STM measurements were performed in a vacuum chamber with a base pressure of 6×10^{-11} Torr. The Cu(111) single-crystal sample was cleaned by repeated cycles of sputtering by 1-keV argon ions and annealing at 600°C. *In situ* electron diffraction showed a well-ordered (1×1) surface. After the final anneal, the sample was allowed to cool down to near room temperature before the STM measurements were made. The STM images were obtained in the constant-current mode to reveal the surface topography.

Figure 1 shows a low-resolution STM picture for an overview over an area of $\sim 1200 \times 1200$ Å². Many line-like features are seen, which are atomic steps. Because of a lack of proper dynamic range for a true grey-scale representation on paper for images with large height variations (such as atomic steps), all of the STM pictures shown in this paper have been processed to filter out the low-spatial-frequency components. As a result,

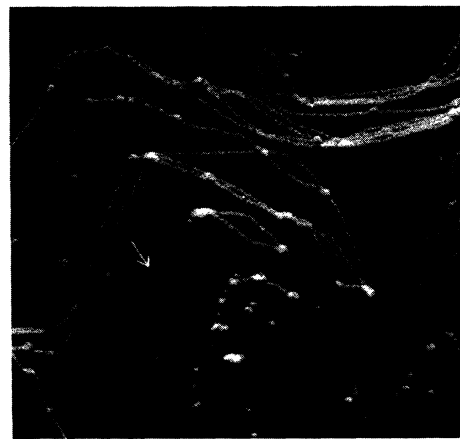


FIG. 1. An STM image of Cu(111) over $\sim 1200 \times 1200$ Å² obtained with a sample bias of 1.4 V and a tunneling current of 0.43 nA. The arrow indicates a place where a dislocation intersects the surface.

only the local height variations are retained, and all of the terraces separated by atomic steps appear equally grey in Fig. 1. The picture resembles a landscape with oblique light illumination from the northern sky, and the steps appear as either bright or dark lines depending on the direction of the step. Most of the steps seen are monatomic steps. Many bumps, mostly at points of intersection of steps and at sharp bends of steps, are observed, which might be associated with irregular Cu structures or impurities either adsorbed on or segregated to the surface during annealing. All of the features seen in Fig. 1 were stable and reproducible over a period of many hours. This particular picture shows a higher-than-average step and bump density.

It is known that metal surfaces, in general, exhibit small surface corrugations and are difficult objects for atomic imaging.¹² The Cu(111) surface is certainly one of the most difficult cases that the authors have encountered due to the relatively small interatomic spacing (2.6 Å). Nevertheless, with careful vibration isolation and under suitable operating conditions of the microscope, it was possible to view the atomic structure in the flat terraces repeatedly. The surface atoms appear as protrusions arranged in a hexagonal net,¹² and neighboring terraces separated by monatomic steps exhibit an offset in the hexagonal net,¹³ corresponding to the ABC stacking sequence of the fcc bulk lattice. A measurement of the step height based on the original unfiltered data yields a step height of $h = 2.1$ Å in agreement with expectation.

The arrow in Fig. 1 indicates the end of a monatomic step; the nearby area forms a section of a spiral surface. An atomic step can end only where a dislocation intersects the surface with a Burgers vector not parallel to the surface. Our survey over a large area on the sample surface shows a dislocation density on the order of $10^{-7}/\text{Å}^2$. In Fig. 1, the bend in the step near the end of the step has no direct bearing on the properties of the dislocation, but serves conveniently as a landmark. Figure 2(a) is a closeup of this dislocation showing atomic resolution (the picture is somewhat distorted by a uniform thermal drift during scanning). The bend in the step can be easily recognized. In taking such an image, tunneling could occur between the side of the STM tip and the step edge just before the tip moves up the step during scanning, because the tip has a finite curvature. This probably explains the fact that we could never resolve all of the atoms right around the step edge. Shown in Fig. 2(b) is a side view of the step profile. This is obtained from the data by subtracting the vertical heights for areas ~ 30 Å to the south of the step from those ~ 30 Å to the north of the step. The west side of Fig. 2(a) is flat, and the step height is zero. The step height begins to build up near the middle of the image, and evolves into a full atomic step height $h = 2.1$ Å near the east border of the image.

The best way to view the atomic misalignment due to

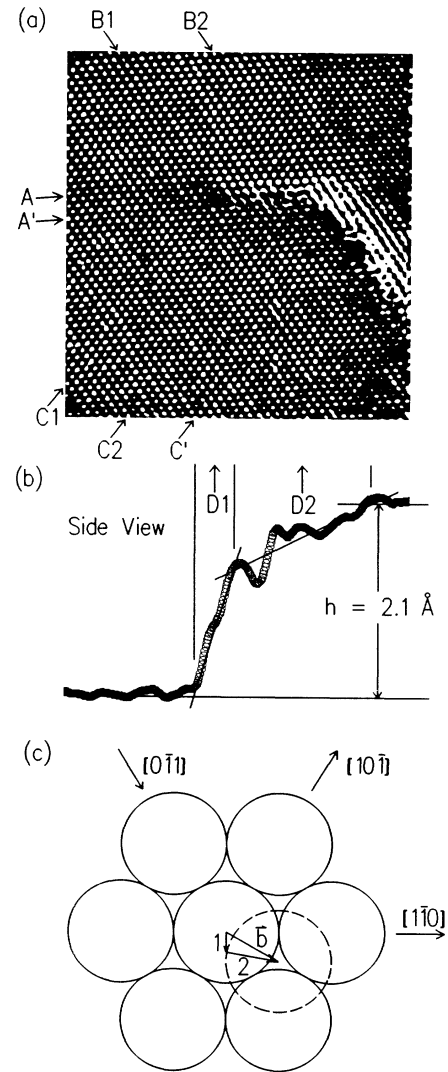


FIG. 2. (a) An STM image of an area encompassing the emergence point of the dislocation shown in Fig. 1. The image was taken with a sample bias of 2 mV and a tunneling current of 4.4 nA. (b) A side view of the step profile obtained by measuring the step height (see text for details). The horizontal scale is the same as that in (a). The circles are data points. The various line segments indicate that the step rise consists of two distinct regions centered about arrows $D1$ and $D2$. (c) Schematic top view of the atomic geometry. The solid-line circles represent close-packed atoms in the (111) plane. The dashed-line circle represents an atom in the layer above. The Burgers vector \mathbf{b} and the partial vectors \mathbf{b}_1 and \mathbf{b}_2 are indicated (they have components out of the page). The main crystallographic directions within the (111) plane are also shown.

dislocations is to sight along the atomic rows at a glancing angle, as described by Kittel in his book using examples of a bubble raft.⁶ If the reader sights along arrow A in Fig. 2(a) from the near to the far side, it is clear that the atomic rows to the left of arrow A are fairly straight.

However, immediately to the right of arrow A the atomic rows show an offset to the right in going across the step. For example, the row labeled by arrow A' shows an offset of about $d/3$ ($d=2.21 \text{ \AA}$ is the inter-row spacing) in going across the step. Similarly, by following the atomic rows starting from around arrow $C1$ to C' , one sees an offset to the right of about $2d/3$ at C' . These observed in-plane offsets along two independent directions, together with the measured vertical step height, allow a unique assignment of the Burgers vector $\mathbf{b} = \frac{1}{2} [101]$ for the dislocation. Figure 2(c) shows schematically a top view of the geometry [for simplicity, a slight tilt of the picture in Fig. 2(a) has been ignored]. The solid-line circles represent close-packed atoms on a (111) plane, and the dashed-line circle represents an atom in the next layer above. The Burgers vector \mathbf{b} , characterizing the slip due to the dislocation, is indicated. Note that the Burgers vector makes an angle of 35.3° to the surface normal. The reader can easily verify that the in-plane offsets (the projections of the Burgers vector) should be $d/3$ and $2d/3$ for sighting along $[1\bar{1}0]$ and $[10\bar{1}]$ (arrows A' and C'), respectively. The above assignment of the Burgers vector is unique in that all other possible choices yield wrong directions for the offsets.

The height evolution in Fig. 2(b) spans a rather large distance, which may seem surprising at first glance. However, it is well known that a dislocation of the type observed here could split up into two partial dislocations (see below).¹⁻⁵ There are two possible geometries; the one appropriate for the present case is $\mathbf{b} = \frac{1}{2} [101] = \mathbf{b}_1 + \mathbf{b}_2 \equiv \frac{1}{6} [112] + \frac{1}{6} [2\bar{1}1]$. The two partial Burgers vectors are shown in Fig. 2(c); the corresponding vertical step heights should be $\frac{2}{3}h$ and $\frac{1}{3}h$, respectively. Figure 2(b) shows that the gradual buildup of the step height consists of two distinct regions centered about arrows $D1$ and $D2$ as indicated, and the height buildup in each region is $\frac{2}{3}h$ and $\frac{1}{3}h$, respectively. Therefore, it appears that the intersecting points of arrows $D1$ and $D2$ with arrow A in Fig. 2(a) are about where the two partial dislocations \mathbf{b}_1 and \mathbf{b}_2 emerge.

To confirm the above proposal, we now check the in-plane strain field around these two partial dislocations along two independent directions. The two arrows $B1$ and $C1$ are drawn to pass through the first partial core. From Fig. 2(c), the in-plane offset caused by \mathbf{b}_1 should be $d/9$ for sighting along both $[10\bar{1}]$ and $[0\bar{1}1]$ (arrows $C1$ and $B1$). Indeed, the atomic rows to the right (left) of arrow $B1$ ($C1$) are fairly straight, but immediately to the left (right) the rows show a small, yet visible, offset of approximately $d/9$ to the left (right) in going across the partial step. Thus, the observed in-plane offsets, together with the measured step height, lead us to conclude that the common intersecting point of arrows A , $B1$, $C1$, and $D1$ is the partial core corresponding to \mathbf{b}_1 . A similar analysis can be made for the other partial dislocation. The two arrows $B2$ and $C2$ indicate the estimated posi-

tion of the second partial core based on the observed in-plane offsets; the arrows A , $B2$, $C2$, and $D2$ all cross one another within one interatomic spacing, as the reader can easily verify. Here, the in-plane offsets are again fairly abrupt in going across the partial core, but it does seem to take a few atomic rows for the offsets to build up fully. This somewhat smeared transition is most likely due to structural relaxation effects. Note that the step-height evolution shown in Fig. 2(b) is also smeared for each partial dislocation (especially for \mathbf{b}_2);¹⁴ in addition to structural relaxation effects, a finite tip radius and tip-surface force interactions could cause such smearing.

The splitting of a dislocation into partial dislocations reduces large abrupt structural distortions and tends to lower the total strain energy. However, a ribbon of stacking fault is formed between the two partial dislocation lines (neither \mathbf{b}_1 nor \mathbf{b}_2 is a lattice vector); this costs energy. The equilibrium separation of the two partials within the bulk is determined by the balance of these two factors, and depends on the character of the dislocation (screw or edge). For the present case of a dislocation intersecting a surface, the most important surface effect is an attractive image force which tends to pull the dislocation line towards the surface. Since the sample is annealed, the dislocation line is likely to be nearly perpendicular to the surface. Thus, the angle α between the dislocation line and the Burgers vector is taken to be about 35° . This implies that the dislocation observed here has a mixed screw and edge character ($\alpha=0^\circ$ and 90° correspond to a pure screw and edge dislocation, respectively). Stobbs and Sworn, in their investigation of a Cu single crystal doped with 0.5% of SiO_2 using the "weak-beam technique" of electron microscopy, deduced the separation between the two partials to be $24 \pm 4 \text{ \AA}$ for $\alpha=35^\circ$;¹¹ this is in excellent agreement with the present result of $25 \pm 2 \text{ \AA}$ obtained from a direct viewing of the atomic positions as seen in Fig. 2.

To summarize, this study demonstrates a useful application of STM. A bulk dislocation intersecting a Cu(111) surface is examined in detail. Atomic positions are viewed in real space, and three-dimensional sub-angstrom resolution of relative atomic displacements is demonstrated.

This Letter was based upon work supported by the U.S. National Science Foundation under Contract No. DMR-8919056. We also acknowledge partial personnel and equipment support by the Shell Oil Company Foundation and the Donors of the Petroleum Research Fund, administered by the American Chemical Society. We acknowledge the use of the central facilities of the Materials Research Laboratory of the University of Illinois, which is supported by the U.S. Department of Energy (Division of Material Sciences, Office of Basic Energy Sciences) under Contract No. DE-AC02-76ER01198, and the U.S. National Science Foundation under Contract No. DMR-8920538.

¹D. Hull, *Introduction of Dislocations* (Pergamon, New York, 1975), 2nd ed.

²W. T. Read, Jr., *Dislocations in Crystals* (McGraw-Hill, New York, 1953).

³F. R. N. Nabarro, *Theory of Crystal Dislocations* (Oxford, London, 1967).

⁴A. H. Cottrell, *Dislocations and Plastic Flow in Crystals* (Oxford, London, 1953).

⁵E. Nadgorny, *Dislocation Dynamics and Mechanical Properties of Crystals* (Pergamon, Oxford, 1988).

⁶C. Kittel, *Introduction to Solid State Physics* (Wiley, New York, 1976), 5th ed., pp. 563–587.

⁷TEM is the best (and perhaps unique) imaging tool for studying dislocations inside a solid; its spatial resolution is comparable to that of STM. The TEM images, however, are not direct images of atoms; a proper interpretation often requires computer simulation. See, for example, M. J. Mills and P. Stadelmann, *Philos. Mag. A* **60**, 355 (1989). This technique has also been applied to surface studies; see, for example, L. D. Marks, *Phys. Rev. Lett.* **51**, 1000 (1983).

⁸See, for example, R. Jayaram and J. A. Spitznagel, *J. Phys. (Paris), Colloq.* **49**, C6-503 (1988); H. C. Eaton, *Phys. Status Solidi (a)* **65**, 497 (1981). Field-ion-microscopy images also show atoms on surfaces, but the technique is limited to very small areas found on a tip. It is difficult to separate boundary effects and to determine atomic positions to subangstrom precision (especially in the direction normal to the surface).

⁹See, for example, N. Osakabe, J. Endo, T. Matsuda, A. To-

nomura, and A. Fukuhara, *Phys. Rev. Lett.* **62**, 2969 (1989); L. M. Peng and J. M. Cowley, *Ultramicroscopy* **29**, 135 (1989). These surface-imaging techniques may have a vertical resolution comparable to that of STM, but the in-plane resolution is much worse.

¹⁰Ch. Wöll, S. Chiang, R. J. Wilson, and P. H. Hippel [*Phys. Rev. B* **39**, 7988 (1989)] described the observation of “stacking-fault dislocations on Au(111).” The dislocation that they referred to is a surface phenomenon, and can be viewed as part of a complex surface reconstruction. Similar stacking-fault-type reconstruction also occurs in the well-known Si(111)-(7×7) system. The dislocation discussed in the present work is a bulk dislocation.

¹¹W. M. Stobbs and C. H. Sworn, *Philos. Mag.* **24**, 1365 (1971); W. M. Stobbs, in *Electron Microscopy in Materials Science (Third Course of the International School of Electron Microscopy)*, edited by U. Valdrè and E. Ruedl (Commission of the European Communities, Luxembourg, 1975), pp. 591–645.

¹²V. M. Hallmark, S. Chiang, J. F. Rabolt, J. D. Swalen, and R. J. Wilson, *Phys. Rev. Lett.* **59**, 2879 (1987).

¹³A. Samsavar, E. S. Hirschorn, F. M. Leibsle, and T.-C. Chiang, *Phys. Rev. Lett.* **63**, 2830 (1989).

¹⁴The response of a metal surface to distortions could also include Friedel-type damped oscillations. Figure 2(b) shows some small oscillatory variations within the region centered about arrow *D2*, which were repeatedly observed.

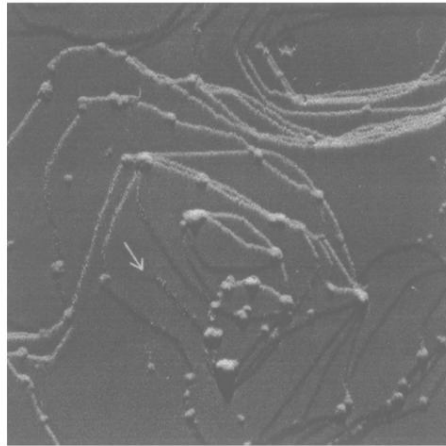


FIG. 1. An STM image of Cu(111) over $\sim 1200 \times 1200 \text{ \AA}^2$ obtained with a sample bias of 1.4 V and a tunneling current of 0.43 nA. The arrow indicates a place where a dislocation intersects the surface.